# Improved Transnasal Transport and Brain Uptake of Tizanidine HCl-Loaded Thiolated Chitosan Nanoparticles for Alleviation of Pain

**DEEPA PATEL, SACHIN NAIK, AMBIKANANDAN MISRA**

TIFAC CORE IN NDDS, Pharmacy Department, Faculty of Technology and Engineering, The Maharaja Sayajirao University of Baroda, Kalabhavan, Vadodara 390001, Gujarat, India

*Received 1 June 2011; revised 8 August 2011; accepted 15 September 2011*

*Published online 17 October 2011 in Wiley Online Library (wileyonlinelibrary.com). DOI 10.1002/jps.22780*

**ABSTRACT:** The aim of this study was to prepare and characterize thiolated chitosan (TC) nanoparticles (NPs) of tizanidine HCl (TZ) and to evaluate its transport across monolayer of RPMI 2650 cells (Human nasal septum carcinoma cell line) followed by assessment of their pharmacokinetic and pharmacodynamic attributes, after intranasal (i.n.) administration. Chitosan was thiolated by carbodiimide method and thiolation was confirmed qualitatively and quantitatively. NPs were prepared using ionotropic gelation and evaluated for mucoadhesion using sheep nasal mucosa for drug permeation and cytotoxicity using monolayer of RPMI 2650 cells. Drug biodistribution was evaluated after technetium-99m labeling, visualized using gamma camera, and evaluated pharmacodynamically by measuring antinociceptive activity in mice. High mucoadhesion and permeation of drug were observed for TC NPs with least toxicity to nasal epithelial cells. Brain uptake and antinociceptive effect of the drug were significantly enhanced after thiolation of chitosan. This concludes that TC NPs, after i.n. administration, show significant increase in the mucoadhesion, reduction in cytotoxicity, enhanced permeation across cells monolayer, higher TZ brain uptake, and considerable increase in antinociceptive activity of TZ in mice. These features make TC an interesting polymer for demonstrating appreciable improvement of transnasal permeation of hydrophilic drugs, such as TZ, known to have limited permeation across blood–brain barrier. © 2011 Wiley Periodicals, Inc. and the American Pharmacists Association J Pharm Sci 101:690–706, 2012

**Keywords:** Chitosan; Nasal Drug Delivery; Nanoparticles; Nasal absorption; Paracellular transport

## INTRODUCTION

Tizanidine HCl (TZ) (molecular weight 290.2 kDa) is a centrally acting skeletal muscle relaxant, used for the symptomatic treatment of painful muscle spasms and spasticity. It is used for the treatment of chronic headache, back pain, and postoperative pain. The major problem associated with oral dosage form of TZ includes low oral bioavailability of about 21% mainly due to extensive first-pass metabolism and its mean elimination half-life of approximately 3 h.[1,2] Hydrophilic natures of conventional therapies are main hindrances due to low permeation through biological barrier. Many novel formulations such as chitosan and thiolated chitosan (TC) nanoparticles (NPs) have been researched nowadays as an alternative to the conventional dosage forms. Intranasal (i.n.) route can deliver a drug to brain bypassing blood–brain barrier (BBB) because of the unique connection between nose and brain. The olfactory pathway

**Abbreviations used:** TZ, tizanidine HCl; NPs, nanoparticles; TC, thiolated chitosan; SA, sodium alginate; SDC, sodium deoxycholate; RB, rhodamine B; LMC, low-molecular-weight chitosan; MMC, medium-molecular-weight chitosan; LMTC, low-molecular-weight thiolated chitosan; MMTC, medium-molecular-weight thiolated chitosan; LMC-TZ NPs, low-molecular-weight TZ-loaded chitosan nanoparticles; MMC-TZ NPs, medium-molecular-weight TZ-loaded chitosan nanoparticles; LMTC-TZ NPs, low-molecular-weight TZ-loaded thiolated chitosan nanoparticles; MMTC-TZ NPs, medium-molecular-weight TZ-loaded thiolated chitosan nanoparticles; LMC-RB NPs, low-molecular-weight rhodamine B-loaded chitosan nanoparticles; MMC-RB NPs, medium-molecular-weight rhodamine B-loaded chitosan nanoparticles; LMTC-RB NPs, low-molecular-weight rhodamine B-loaded thiolated chitosan nanoparticles; MMTC-RB NPs, medium-molecular-weight rhodamine B-loaded thiolated chitosan nanoparticles.

Additional Supporting Information may be found in the online version of this article. Supporting Information

*Correspondence to*: Ambikanandan Misra (Telephone: +91-265-2434187; Fax: +91-265-2423898; E-mail: misraan@sify.com)

Journal of Pharmaceutical Sciences, Vol. 101, 690–706 (2012)

provides a superior option for brain targeting.[3] Mucoadhesive NPs via i.n. route significantly increase the mucosal absorption and the residence time by reducing the mucociliary clearance in the nasal cavity.[3] In addition, nanoparticles may able to cross the mucosal epithelium better than microparticles.[4,5] Along with the various available bioadhesive materials, chitosan has been anticipated for nasal delivery of drugs. Chitosan is a copolymer of glucosamine and N-acetyl glucosamine and has received attention as a mucoadhesive agent. Chitosan is bioadhesive, biodegradable, and low toxic pharmaceutical excipient for drug delivery systems.[6] Moreover, chitosan has an ability to facilitate paracellular transport of hydrophilic drugs across mucosa.[7–9] In spite of several advantages, chitosan has a major disadvantage of insolubility at physiological pH.[9] It can solubilize and get activated as an absorption enhancer only when it protonates in acidic environments.

Thiolation of chitosan can provide much higher mucoadhesive properties than chitosan and its higher mucoadhesive properties can be explained by the formation of covalent bonds between the thiol group and the mucus glycoprotein. This covalent bond formation is stronger than noncovalent bonds between the chitosan and mucus glycoprotein. TC can interact with cysteine residue of mucus glycoproteins via oxidation or disulfide exchange reactions.[10] This TC has several advantageous features in comparison with chitosan, such as significantly improved permeation and mucoadhesive properties. Moreover, soluble TC displays *in situ* gelling properties at physiological pH.[11,12] With chitosan–thioglycolic acid (TGA) conjugates, a fivefold to 10-fold increase in mucoadhesion in comparison with unmodified chitosan was achieved.[13]

The aim of this study was to prepare and characterize TC NPs of TZ and to evaluate its transport across monolayer of Roswell Park Memorial Institute (RPMI) 2650 cells followed by assessment of their pharmacokinetic and pharmacodynamic attributes, after i.n. administration.

## MATERIALS AND METHODS

### Materials

Tizanidine HCl was a gift sample from Endoc Pharma (Rajkot, Gujarat, India). Chitosan [low (60 kDa)- and medium-molecular weight (450 kDa)], sodium deoxycholate (SDC), and Rhodamine B (RB) were purchased from Sigma–Aldrich (Bangalore, Karnataka, India). RMPI 2650 cell line was procured from National Centre for Cell Science (Pune, Maharashtra, India). Eagle's minimum essential medium (MEM), N-2-hydroxyethylpiperazine-N′-2-ethanesulfonic acid (HEPES), Hank's balanced salt solution (HBSS), and 1-ethyl-3-(3-dimethylaminopropyl) carbodiimide (EDC) hydrochloride were purchased form the Himedia (Mumbai, Maharashtra, India). TGA and acetonitrile [high-performance liquid chromatography (HPLC) grade] were purchased from the Merck (Mumbai, Maharashtra, India). Sodium alginate (SA) was purchased from the National Chemical Laboratory (Mumbai, Maharashtra, India). Acetic acid and other analytical reagents were obtained from SD. Fine Chemicals Limited (Vadodara, Gujarat, India), and all the reagents used were of analytical grade. The 12-well culture plate inserts (0.4-μm pore size, 30-mm diameter, polycarbonate) were purchased from Millipore Corporation (Bedford, Massachusetts).

### Methods

#### *Preparation of TC*

Thiolated chitosan was synthesized by previously reported method.[14] Around 500 mg of chitosan each (low- and medium-molecular weight) was dissolved in 50 mL of 1.0% acetic acid and then 100 mg of EDC was added in chitosan solution. After solubilization of EDC, 30 mL of TGA was added. The pH of the reaction mixture was adjusted to 5.0 with 3 N NaOH and reaction mixture was stirred for 3 h at room temperature. Afterward, the reaction mixture was dialyzed five times against 5 mM HCl using dialysis bag (molecular weight cutoff 10 kDa) over a period of 3 days in the dark for the removal of unbound TGA and to separate the polymer conjugates. After 3 days again, reaction mixture was dialyzed two times against 5 mM HCl containing 1.0% NaCl for the reduction of ionic interactions between the cationic polymer and the anionic sulfhydryl compound.[14] Thiol groups in TC were analyzed quantitatively by "Ellman's method" and qualitatively confirmed by Fourier transform infrared spectroscopy.

#### *Preparation of TZ-Loaded Chitosan and TC NPs*

Particles from chitosan were prepared by ionic gelation of chitosan with SA. Briefly, chitosan (1, 1.5, and 2 mg/mL) was dissolved in 1% acetic acid solution. After stirring overnight, the drug (1, 2.5, and 4 mg/mL) was added in chitosan solution. SA (0.5, 1, and 1.5 mg/mL) solution was added dropwise to above chitosan solution to form different ratio of chitosan to SA solutions, under moderate stirring. Following stirring for 20 min, the particle suspension was centrifuged at 4°C at 19051 g for 30 min.[15] Particles from TC were prepared by ionic gelation of TC using SA with slight modification in above-mentioned method. TC (1, 2, and 3 mg/mL) was dissolved in distilled water. Different concentration of drug solution (1, 2, and 3 mg/mL) was incubated with SDC solution (5, 10, and 15 mg/mL) for 30 s. The resulting complex was added to TC

solution. Then, SA solution (0.25, 0.5, and 0.75 mg/mL) was added dropwise, with stirring to the above TC mixture in order to form different ratio of TC solution–SA solution–SDC solution–drug solution, which led to the immediate formation of NPs. The particle suspension was centrifuged at 4°C at 18,000 rpm for 30 min.[16] The NPs were washed and subjected to characterization for zeta potential, particle size, and drug entrapment. The supernatant was analyzed for entrapment efficiency using HPLC. From various ratios of chitosan solution–SA solutions (2:1, 3:1, and 4:1), chitosan NPs batch that gives maximum entrapment efficiency and minimum size was selected. In case of TC NPs, the ratios of TC solution–SA solution–drug solution–SDC solution were kept as 7:1:1:1, 4:2:2:2, and 5.5:1.5:1.5:1.5. The impact of chitosan solution pH (4 and 5) and SA solution pH (8, 9, 10, and 11) was seen on the effect of particle size and drug entrapment for optimal formulation of chitosan NPs.[17,18]

## Characterizations

### *Characterization of TC*

*Procedure for Quantitating Sulfhydryl Groups Based on Molar Absorptivity (Ellman's Method).* Thiol groups in TC were analyzed quantitatively by "Ellman's method."[14] Reaction buffer (0.1 M sodium phosphate, pH 8, containing 1 mM ethylenediaminetetraacetic acid) was used for the preparation of TC solution and Ellman's reagent. For each polymer sample to be tested, 50 μL of Ellman's reagent solution (4 mg Ellman's reagent in 1 mL of reaction buffer), 2.5 mL of reaction buffer, and 250 μL of each polymer solution (low- and medium-molecular-weight TC solutions) was added to the separate test tubes. As a blank, 250 μL of reaction buffer was processed. Finally, the mixture was incubated at room temperature for 15 min and absorbance was measured at 412 nm using spectrophotometer. The amount and concentration of sulfhydryls in the sample were calculated from the molar extinction coefficient of 2-nitro-5-thiobenzoic acid (14,150 $M^{-1}cm^{-1}$).

*Infrared Spectra of Chitosan and TC.* Infrared spectra of different molecular weight chitosan and TC were obtained and analyzed for confirmation of the thiol group (Fig. 1).

### *Characterization of Chitosan and TC NPs*

*Particle Size.* The particle size and particle size distribution of NPs dispersion were determined using dynamic light scattering with a Malvern Zetasizer (NanoZS; Malvern Instruments, Malvern, Warcestershire, UK). The particle size of each NPs formulation was tabulated in Table 1.

**Table 1.** Characterization of Optimized Chitosan, Thiolated Chitosan NPs Formulations

| Formulation | Chitosan/Thiolated Chitosan (mg/mL) | SA (mg/mL) | Drug (mg/mL) | SDC (mg/mL) | Ratio | Particle Size (nm) | Zeta Potential (mV) | Entrapment Efficiency (%) |
|---|---|---|---|---|---|---|---|---|
| LMC-TZ NPs | 1 (pH 5) | 0.5 (pH 9) | 2.5 | – | Chitosan solution to SA solution (2:1) | 473.5 ± 13.5 | 22.8 ± 0.876 | 44.69 ± 3.5 |
| MMC-TZ NPs | 1 (pH 5) | 0.5 (pH 9) | 2.5 | – | Chitosan solution to SA solution (2:1) | 598.7 ± 1.8 | 23.8 ± 0.987 | 46.65 ± 2.4 |
| LMTC-TZ NPs | 2 | 0.5 | 2 | 10 | Thiolated chitosan–SA–drug–SDC solution (7:1:1:1) | 262.5 ± 12.4 | 12.9 ± 1.44 | 68.8 ± 6.34 |
| MM TC-TZ NPs | 2 | 0.5 | 2 | 10 | Thiolated chitosan–SA–drug–SDC solution (7:1:1:1) | 264.9 ± 15 | 14.5 ± 1.1 | 72.2 ± 3.4 |
| LMC-RB NPs | 1 (pH 5) | 0.5 (pH 9) | 2.5 | – | Chitosan solution to SA solution (2:1) | 463.9 ± 18.1 | 21.3 ± 0.763 | 40.34 ± 2.5 |
| MMC-RB NPs | 1 (pH 5) | 0.5 (pH 9) | 2.5 | – | Chitosan solution to SA solution (2:1) | 621.8 ± 16.8 | 24.8 ± 0.988 | 63.78 ± 4.3 |
| LMTC-RB NPs | 2 | 0.5 | 2 | 10 | Thiolated chitosan–SA–RB–SDC solution (7:1:1:1) | 262.9 ± 15.9 | 17.8 ± 2.1 | 65.89 ± 3.1 |
| MMTC-RB NPs | 2 | 0.5 | 2 | 10 | Thiolated chitosan–SA–RB–SDC solution (7:1:1:1) | 276.2 ± 13.9 | 18.3 ± 1.4 | 75.57 ± 4.1 |

(Mean ± SD, $n = 3$)
LMC-TZ NPs, low-molecular-weight tizanidine HCl-loaded chitosan nanoparticles; MMC-TZ NPs, medium-molecular-weight tizanidine HCl-loaded chitosan nanoparticles; LMTC-TZ NPs, low-molecular-weight tizanidine HCl-loaded thiolated chitosan nanoparticles; MMTC-TZ NPs, medium-molecular-weight tizanidine HCl-loaded thiolated chitosan nanoparticles; LMC-RB NPs, low-molecular-weight rhodamine B-loaded chitosan nanoparticles; MMC-RB NPs, medium-molecular-weight rhodamine B-loaded chitosan nanoparticles; LMTC-RB NPs, low-molecular-weight rhodamine B-loaded thiolated chitosan nanoparticles; MMTC-RB NPs, medium-molecular-weight rhodamine B-loaded thiolated chitosan nanoparticles.


DOI 10.1002/jps

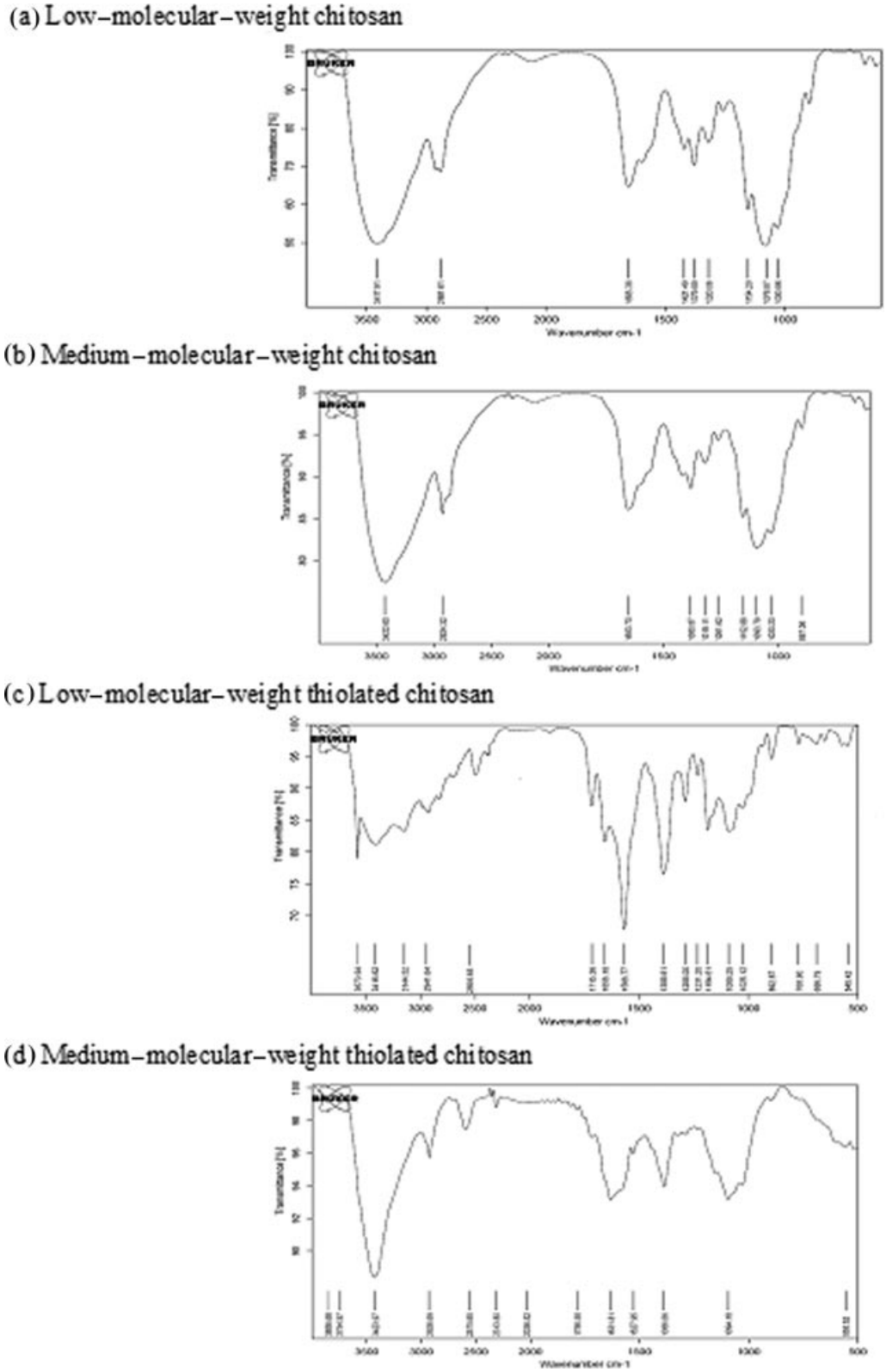


**Figure 1.** Infrared spectra. (a) low-molecular-weight chitosan, (b) medium-molecular-weight chitosan, (c) low-molecular-weight thiolated chitosan, and (d) medium-molecular-weight thiolated chitosan.

*Zeta Potential.* Zeta potential measurement of NPs dispersion was performed using a Malvern Zetasizer (NanoZS; Malvern Instruments). The zeta potential of each NPs formulation was tabulated in Table 1.

*Encapsulation Efficiency or Percentage Drug Entrapment.* Drug-loaded NPs suspension was diluted with 1% (v/v) acetic acid solution, sonicated for 30 min, and filtered through 0.22 μm microporous membrane. The total drug loading into NPs formulations was determined by measuring the drug content in the filtrate using HPLC. The entrapment efficiency was determined upon separation of NPs from the aqueous suspension containing nonentrapped drug using centrifugation at 18,000 rpm at 4°C for 30 min. The amount of free drug in the supernatant was measured by HPLC.[19] The drug was estimated using a Shimadzu HPLC system (Shimadzu, Japan). The HPLC system was composed of a pump (LC-20AT prominence, Shimadzu), a sample 20-μL loop injector (Rheodyne 7725), and an ultraviolet (UV)–visible spectrophotometric detector (SPD-20A prominence, Shimadzu). The separation was carried out on a Phenomenex $C_{18}$ (250 × 4.6 mm) HPLC column (Phenomenex) having particle size of 5 μm. Mobile phase for TZ consisted of acetonitrile–water (80:20), UV detection was at 241 nm, and mobile phase flow rate was 1 mL/min. The retention time of TZ was about 5.73 min. Drug entrapment efficiency (%EE) in the drug-loaded NPs was calculated according to the equation below:

$$\%\,\mathrm{EE} = \frac{\text{Total amount of drug loading} - \textit{F}\text{ree drug in supernant}}{\text{Total amount of drug loading}} \times 100$$

The %EE of each NPs formulation was tabulated in Table 1.

*Transmission Electron Microscopy.* Transmission electron microscopy (TEM) images were taken by the transmission electron microscope (Morgagni, Philips, the Netherlands) using negative staining (2% phosphotungstic acid). TEM images of each formulation were shown in Figure 2.

*Confocal Laser Scanning Microscopy Examination.* Rhodamine B-loaded chitosan and TC NPs were used for the confocal microscopy examination. RB-loaded chitosan and TC NPs were prepared same as the drug-loaded chitosan and TC NPs. The particle size, zeta potential, and drug entrapment of RB-loaded NPs were similar to the drug-loaded NPs (Table 1). For confocal laser scanning microscopy examinations, sheep nasal mucosa was rinsed with phosphate buffer saline (pH 6.4) twice; the freshly excised nasal mucosa was placed in a petri dish. One milliliter of the fluorescent probes RB-loaded NPs dispersions in PBS

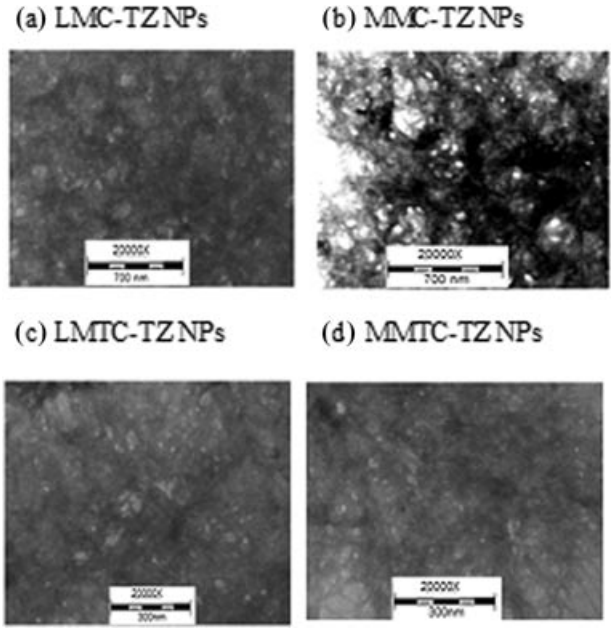


**Figure 2.** TEM images.

(pH 6.4) (10 mg/mL NPs dispersion of chitosan and TC) was added to the mucosal surface and incubated for 20 min at 37.8°C. After incubation, the treated mucosa was washed gently with phosphate buffer saline (pH 6.4) to remove the excess NPs. The sample was then mounted on a glass slide and immediately examined under confocal microscope. Fluorescent images were obtained using an upright confocal laser scanning microscope (LSM510, Carl Zeiss, Germany) equipped with 543 nm excitation laser HeNe1 and emission long pass filter 560 nm (LP560).[20] Figure 3 shows the confocal image of mucosal surface and Figure 4 shows the confocal image after Z sectioning of nasal mucosa for RB solution, RB-loaded chitosan NPs, and RB-loaded TC NPs.

### *Transepithelial Electrical Resistance Measurement and Permeation Studies of TZ Solution and TZ-Loaded Chitosan and TC NPs*

*TEER Measurement.* RPMI 2650 cells were seeded at a density of $5 \times 10^5$ cells per well into 12-well culture plates in Eagle's MEM supplemented with 10% fetal bovine serum (FBS) and 50 μg/mL penicillin and streptomycin. The cells were incubated for 2 days at 37°C in 95% air and 5% $CO_2$. Transepithelial electrical resistance (TEER) of RPMI 2650 cells across cell monolayer was measured at 24-h intervals until the cells form confluent monolayer using Millicell® ERS meter (Millipore Corporation). Cell monolayer TEER was measured by subtracting the background resistances of blank RPMI 2650 cells. TEER readings increased subsequently indicating that the cells formed tight junction and formed a close packing.

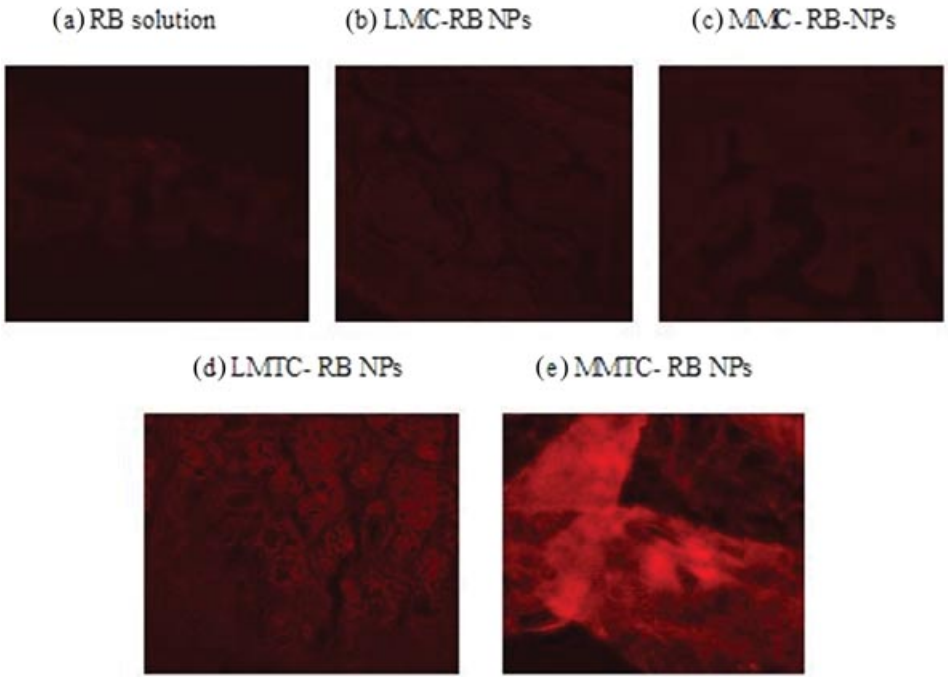


**Figure 3.** Confocal images of (a) RB solution, (b) LMC-RB NPs, (c) MMC-RB NPs, (d) LMTC-RB NPs, and (e) MMTC-RB NPs.

The value of TEER at $t = 0$ h time was taken as 100% (initial values) and the TEER values at each sampling time (0, 30, 60, and 150 min) point were expressed as percent of initial values. After 150 min of incubation, the formulations were replaced by HBSS–HEPES buffer to determine the recovery of TEER to its initial value.[21–23]

*Permeation Studies.* Before starting the permeation experiment, the culture media were removed from both apical (AP) and basolateral (BL) sides of the cell monolayers and the cell monolayer was washed with fresh HBSS buffered with 30 mM HEPES (37 ± 1°C) and replaced with phosphate buffer saline (pH 7.4) and equilibrated for 30 min. TEER measurement and permeation study were carried out on the AP to BL direction by adding TZ-loaded TC NPs (equivalent to 2 mg/mL of drug) and TZ-loaded chitosan NPs (equivalent to 2 mg/mL of drug), TZ solution (2 mg/mL of drug) on the AP side and 2.5 mL of phosphate buffer saline (pH 7.4) on BL side. A 2.5 mL of sample was collected from the receiver (BL) side at different time intervals (0, 30, 60, and 150 min) and replaced with 2.5 mL of fresh (37 ± 1°C) phosphate buffer saline (pH 7.4) for maintenance of sink conditions at the same time intervals. Collected sample was immediately analyzed for the drug using HPLC. Permeation studies were carried out by placing the well plates on a calibrated shaker at 50 rpm at 37°C.[21–23]

Apparent permeability coefficient ($P_{app}$) values of all the formulations were calculated using Eq. 1 and results were tabulated and recorded in Tables 2 and 3.

$$P_{app} = [(dQ/dt) \times (V_R/A \times C_0)] \quad (1)$$

where $P_{app}$, apparent permeability coefficient (cm/s); $dQ/dt$, cumulative flux in the AP to BL direction (μg/s); $V_R$, volume of the receptor compartment ($cm^3$); $A$, diffusion area of the monolayer (3.8 $cm^2$); $C_0$, initial concentration applied on the AP side (μg/s).

The data were statistically analyzed using one-way analysis of variance (ANOVA) and differences between groups were found to be $p < 0.05$.

*Cell Viability Study.* The cytotoxicity of the chitosan/TC and drug-loaded chitosan/TC NPs was determined on differentiated RPMI 2650 cells. RPMI 2650 cells were seeded at a density of $5 \times 10^3$ cells per well into 96-well culture plates in Eagle's MEM (the MEM was supplemented with 10% FBS and 50 μg/mL penicillin and streptomycin) and then incubated for 2 days at 37°C in 95% air and 5% $CO_2$. HBSS buffered with 30 mM HEPES (pH 7.2, adjusted with 0.1 M NaOH) was used as a vehicle for preparation of formulations. The cells were exposed to HBSS–HEPES buffer, soluble chitosan, soluble TC, drug-loaded chitosan, and TC NPs in HBSS–HEPES with different concentration and incubated at 37°C for 2 h. Thereafter, the NPs formulations and polymers were removed and gently washed with HBSS–HEPES buffer and replaced by 100 μL MEM and 20 μL of 3-(4,5-dimethylthiazol-2-yl)-2,5-diphenyltetrazolium bromide (MTT), a

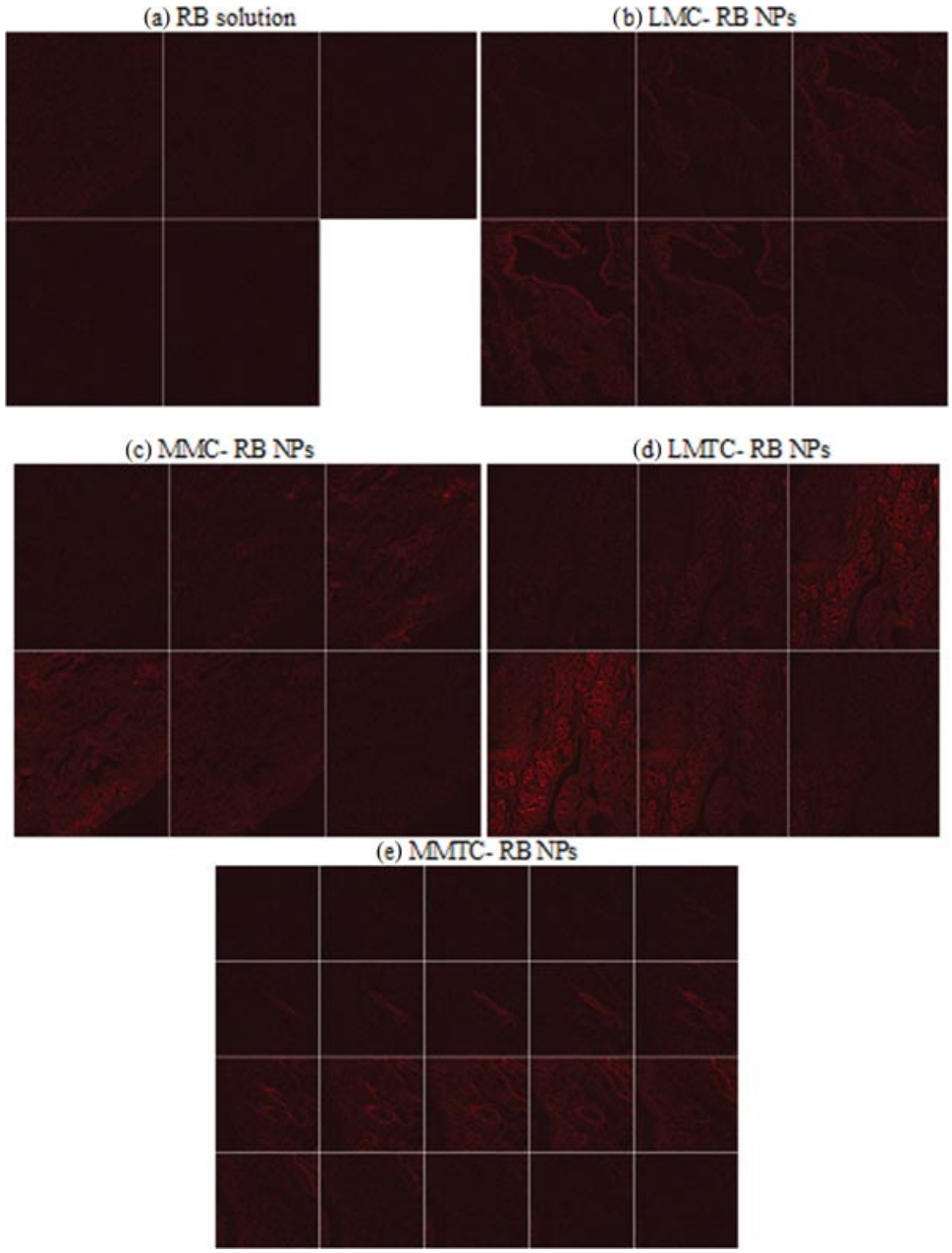


**Figure 4.** Confocal images after Z sectioning of nasal mucosa. (a) RB solution, (b) LMC-RB NPs, (c) MMC-RB NPs, (d) LMTC-RB NPs, and (e) MMTC-RB NPs.

**Table 2.** TEER Values of RPMI 2650 Cell Monolayer at Different Time Intervals

| | Transepithelial Electrical Resistance Value ($cm^2$)[a] | | | | |
|---|---|---|---|---|---|
| Time | TZ solution | LMC-TZ NPs | MMC-TZ NPs | LMTC-TZ NPs | MMTC-TZ NPs |
| 30 min | 98.32 ± 5.3 | 56.34 ± 3.7 | 62.78 ± 2.9 | 42.87 ± 3.1 | 47.90 ± 2.8 |
| 60 min | 89.45 ± 6.3 | 50.98 ± 2.3 | 57.32 ± 2.1 | 37.89 ± 2.4 | 43.87 ± 1.6 |
| 150 min | 78.34 ± 4.1 | 46.21 ± 2.2 | 49.43 ± 1.5 | 31.32 ± 1.7 | 34.89 ± 1.4 |
| Recovery after 150 min | 96.87 ± 3.2 | 59.01 ± 3.8 | 61.11 ± 4.2 | 96.57 ± 5.1 | 96.89 ± 4.9 |

[a]Transepithelial electrical resistance values are expressed as percent of initial values ($p < 0.05$). Mean ± SD, $n = 3$.

 DOI 10.1002/jps

**Table 3.** Apparent Permeability Coefficients ($P_{app}$) of TZ Formulations Across the RPMI 2650 Cell Monolayer

| Formulations | Apparent Permeability Coefficients ($P_{app}$) $\times 10^{-6}$ cm/s |
|---|---|
| TZ solution | 0.674 ± 0.032 |
| LMC-TZ NPs | 9.43 ± 0.367 |
| MMC-TZ NPs | 8.67 ± 0.495 |
| LMTC-TZ NPs | 19.76 ± 0.678 |
| MMTC-TZ NPs | 18.43 ± 0.564 |

$p < 0.05$.
Mean ± SD, $n = 3$.
LMC-TZ NPs, low–molecular-weight tizanidine HCl-loaded chitosan nanoparticles; MMC-TZ NPs, medium-molecular-weight tizanidine HCl-loaded chitosan nanoparticles; LMTC-TZ NPs, low-molecular-weight tizanidine HCl-loaded thiolated chitosan nanoparticles; MMTC-TZ NPs, medium-molecular-weight tizanidine HCl-loaded thiolated chitosan nanoparticles.

tetrazole (5 mg/mL). Cells were incubated for at 37°C for 2 h. To dissolve formazane crystals formed, the MTT solution was removed and replaced with 100 µL of dimethyl sulfoxide per well and kept in incubator for 10 min at 37°C in 95% air and 5% $CO_2$ and afterward, 15 min at 6°C before analysis. Finally, the absorbance was measured at 570 nm with the reference filter of 655 nm using enzyme-linked immunosorbent assay reader. The data were statistically analyzed using one-way ANOVA.[22] Figure 5 shows the cell viability study of polymers and NPs formulations.

## *In Vivo* Study

### *Biodistribution Studies*

The biodistribution study on Swiss albino mice (20–25 g and aged 16–20 weeks) was approved and performed in accordance by the Social Justice and Empowerment Committee for the purpose of control and supervision on animals and experiments, Ministry of Government of India. Biodistribution studies were performed by administration of $^{99m}$Tc (technetium)-labeled NPs and drug solutions through i.n. route, intravenous (i.v.), and oral routes in Swiss albino mice, and drug brain targeting efficiency was compared among three routes of administration. The radiochemical purity of $^{99m}$Tc–TZ solution/$^{99m}$Tc–TZ-loaded chitosan NPs [$^{99m}$Tc–LMC (low-molecular-weight chitosan)–TZ NPs and $^{99m}$Tc–MMC (medium-molecular-weight chitosan)–TZ NPs] and $^{99m}$Tc–TZ-loaded TC NPs [$^{99m}$Tc–LMTC (low-molecular-weight TC)–TZ NPs and $^{99m}$Tc–MMTC (medium–molecular-weight TC)–TZ NPs] were assessed using ascending instant thin layer chromatography (ITLC). Silica gel-coated fiber glass sheets (Gelman Sciences, Inc., Ann Arbor, Michigan) and dual solvent systems consisting of acetone and pyridine–acetic acid–water (3:5:1.5, v/v) were used as mobile phase. The radiolabeling was optimized by taking three factors in consideration: amount of stannous chloride, incubation time, and *in vitro* stability of radiolabeled complex in normal saline and mice serum. The pH and bonding strength [optimized amount of diethylenetriaminepentaacetic acid (DTPA)] were also optimized for optimum labeling. For biodistribution study, the animals were held in slanted position and formulations ($^{99m}$Tc-labeled–TZ solution equivalent to 0.00104 mg/g of TZ and $^{99m}$Tc-labeled–TZ-loaded chitosan/TC NPs equivalent to 0.00104 mg/g of TZ) were administered through i.v., i.n., and oral route in mice. Formulations were instilled into nostrils (10 µL in each nostril) with the help of micropipette (10–100 µL) attached with low-density polyethylene tubing internal diameter of 0.1 mm at the delivery site for i.n. administration. Before proceeding i.n. administration, the mice were anesthetized by intramuscular injection of ketamine (50 mg/kg). The animals were killed humanely at different time intervals (0.5, 1, 2, 4, and 8 h) and the

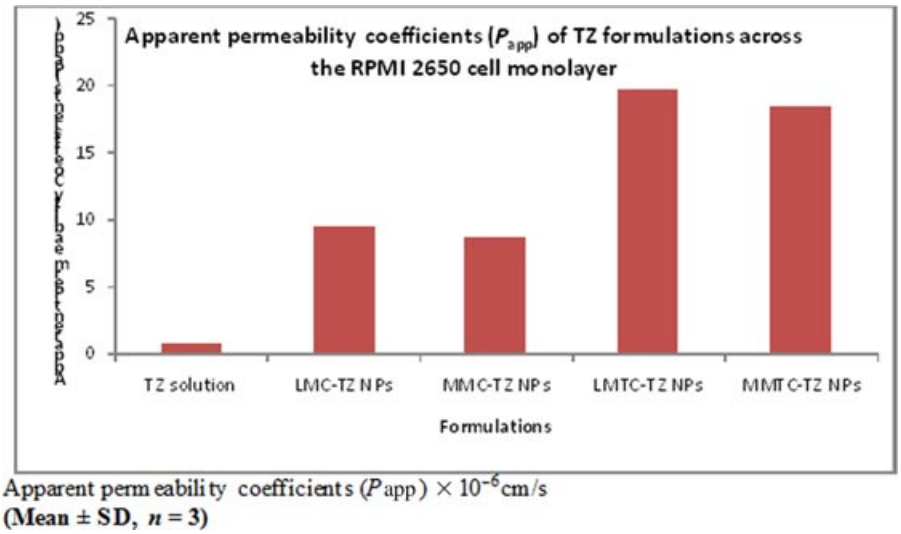


**Figure 5.** Cell viability study of chitosan, thiolated chitosan, and its NPs formulations.

blood was collected using cardiac puncture. Consequently, brain and other tissues (liver, kidney, spleen, tail, stomach, and intestine) (Supplementary Table 1 & 2) were dissected, washed with normal saline to remove adhering tissue/fluid, weighed, and measured the radioactivity present in each tissue/organ using gamma scintillation counter. The uptake of radiopharmaceutical per gram in each tissue/organ was calculated as a fraction of administered dose.[24] The blood–brain ratio of TZ formulations is tabulated in Table 4. Table 5 shows the pharmacokinetic parameters of TZ formulation calculated using Kinetica software. The degree of drug targeting to brain after i.n. administration can be evaluated by the drug targeting index (DTI). DTI was derived from the ratio of the value of Area under the curve ( $AUC)_{brain}$/Area under the curve $(AUC)_{blood}$ following i.n. administration to that following i.v. injection. The higher the value of DTI, more is the degree of drug targeting efficiency to brain after i.n. administration, and DTI can be determined using the following equation[24]:

$$DTI = \frac{(AUC_{brain\,tissue}/AUC_{blood})_{i.n.}}{(AUC_{brain\,tissue}/AUC_{blood})_{i.v.}}$$

Moreover, to understand the direct nose to brain transport after i.n. administration, the drug targeting percentage (DTP) was introduced, the equation is given below:

$$DTP\,(\%) = \frac{B_{i.n.} - B_x}{B_{i.n.}} \times 100$$

where $B_x = (B_{iv.}/P_{i.v.}) \times P_{i.n.}$,where $B_x = AUC_{brain}$ fraction that contributed by systemic circulation through the BBB following intranasal delivery. $B_{i.v.} = AUC_{brain}$ following i.v. administration; $P_{i.v.} = AUC_{blood}$ after i.v. administration; $B_{i.n.} = AUC_{brain}$ flowing intranasal delivery; $P_{i.n.} = AUC_{blood}$ by intranasal administration.

Statistical differences between two route of administration (i.n. and i.v.) were complete using the unpaired Student's $t$-test and a value of $p < 0.05$ was considered statistically significant. Results were presented as mean values ± SD.

**Table 4.** Blood–Brain Ratio of $^{99m}$TC–LMC-TZ NPs/MMC-TZ NPs/LMTC-TZ NPs/MMTC-TZ NPs/$^{99m}$TC–TZ Solution in Swiss Albino Mice at Predetermine Time Intervals of Intranasal Administration

| Time (h) | Brain–Blood Ratio |
|---|---|
| Intranasal Administration of $^{99m}$TC–LMC-TZ NPs | |
| 0.5 | 1.095870206 |
| 1 | 0.559649123 |
| 2 | 0.183244681 |
| 4 | 0.211235955 |
| 8 | 0.321965898 |
| Intranasal Administration of $^{99m}$TC–MMC-TZ NPs | |
| 0.5 | 0.542011834 |
| 1 | 0.644117647 |
| 2 | 0.25877551 |
| 4 | 0.238565022 |
| 8 | 0.482972136 |
| Intranasal Administration of $^{99m}$TC–LMTC-TZ NPs | |
| 0.5 | 1.784660767 |
| 1 | 1.563636364 |
| 2 | 0.931818182 |
| 4 | 1.1834962 |
| 8 | 2.5546875 |
| Intranasal Administration of $^{99m}$TC–MMTC-TZ NPs | |
| 0.5 | 1.942771084 |
| 1 | 1.675025075 |
| 2 | 0.921875 |
| 4 | 1.207464325 |
| 8 | 2.644351464 |
| Intravenous Administration of $^{99m}$TC–TZ Solution | |
| 0.5 | 0.000757002 |
| 1 | 0.006421152 |
| 2 | 0.033333333 |
| 4 | 0.023783784 |
| 8 | 0.004081633 |
| Oral Administration of $^{99m}$TC–TZ Solution | |
| 0.5 | 0.444444444 |
| 1 | 0.114551084 |
| 2 | 0.059753954 |
| 4 | 0.30449827 |
| 8 | 0.112359551 |
| Intranasal Administration of $^{99m}$TC–TZ Solution | |
| 0.5 | 0.05492228 |
| 1 | 0.297474747 |
| 2 | 0.088974359 |
| 4 | 0.072302158 |
| 8 | 0.035860656 |

Mean ± SD, $n = 3$.

### *Gamma Scintigraphy Imaging*

The Swiss albino mice (20–25 g and aged 16–20 weeks) were anesthetized using ketamine injection prior to administration of radiolabeled formulations. The animals were held from back in slanted position and formulations were ($^{99m}$Tc–TZ containing 0.00104 mg/g of TZ and similarly, $^{99m}$Tc–TZ-loaded chitosan/TC NPs containing 0.00104 mg/g of TZ) administered through i.v., i.n., and oral route in Swiss albino mice. The formulations were instilled into nostrils (10 μL in each nostril) with the help of micropipette (10–100 μL) attached with low-density polyethylene tubing with internal diameter of 0.1 mm at the delivery site for i.n. administration. Then, the anesthetized animals were placed on board and images were captured using gamma camera. Imaging was performed using single-photon emission computerized tomography (LC 75-005, Diacam; Siemens AG, Erlanger, Germany) gamma camera.[24] Figure 6 shows the gamma scintigraphy imaging of TZ-loaded chitosan NPs, TC NPs, and TZ solution following i.v., oral, and i.n. administrations.

### *Pharmacodynamic Study*

Swiss albino mice weighing between 20 and 25 g (aged 16–20 weeks) were selected randomly for the

**Table 5.** Pharmacokinetics of $^{99m}$TC–TZ solution/LMC-TZ NPs/MMC-TZ NPs/LMTC-TZ NPs/MMTC-TZ NPs

| Formulation | Organ/Tissue | $C_{max}$ (% radio actvity/g) | $T_{max}$ (h) | $AUC_{0\rightarrow 8h}$ (h × %radioactivity/g) | $T_{1/2}$ (h) | MRT | DTI | DTP (%) |
|---|---|---|---|---|---|---|---|---|
| TZ solution (i.v.) | Blood | 10.59 | 0.5 | 44.26 | 3.06 | 4.06 | – | – |
| | Brain | 0.189 | 2 | 1.05 | 3.9 | 0.189 | | |
| TZ solution (oral) | Blood | 0.569 | 2 | 2.4 | 2.25 | 4.3 | | – |
| | Brain | 0.088 | 2 | 0.301 | 1.95 | 3.95 | – | |
| TZ solution (i.n.) | Blood | 3.9 | 2 | 21.61 | 2.9 | 5.32 | | 70.82 |
| | Brain | 0.589 | 1 | 1.755 | 1.75 | 3.14 | 3.42 | |
| LMC-TZ NPs | Blood | 3.76 | 2 | 21.18 | 3.08 | 5.56 | | 92.25 |
| | Brain | 0.957 | 1 | 6.75 | 5.36 | 8.07 | 13.43 | |
| MMC-TZ NPs | Blood | 3.45 | 2 | 16.093 | 2.44 | 4.72 | | 94.21 |
| | Brain | 0.876 | 1 | 6.59 | 5.75 | 8.62 | 17.26 | |
| LMTC-TZ NPs | Blood | 1.32 | 2 | 6.96 | 2.47 | 4.46 | | 98.97 |
| | Brain | 1.72 | 1 | 14.08 | 6.38 | 9.48 | 85.23 | |
| MMTC-TZ NPs | Blood | 1.26 | 2 | 6.64 | 2.41 | 4.42 | | 98.78 |
| | Brain | 1.67 | 1 | 12.91 | 5.49 | 8.45 | 81.95 | |

study. The animals were divided in groups of five animals. The formulations (TZ solution/low-molecular-weight TZ-loaded chitosan nanoparticles (LMC-TZ NPs)/medium-molecular-weight TZ-loaded chitosan nanoparticles (MMC-TZ NPs)/low-molecular-weight TZ-loaded thiolated chitosan nanoparticles (LMTC-TZ NPs)/MMTC-TZ NPs equivalent to 0.00104 mg/g of TZ) were administered in 10 μL in each nostril using micropipette (10–100 μL) attached with low-density polyethylene tubing with internal diameter of

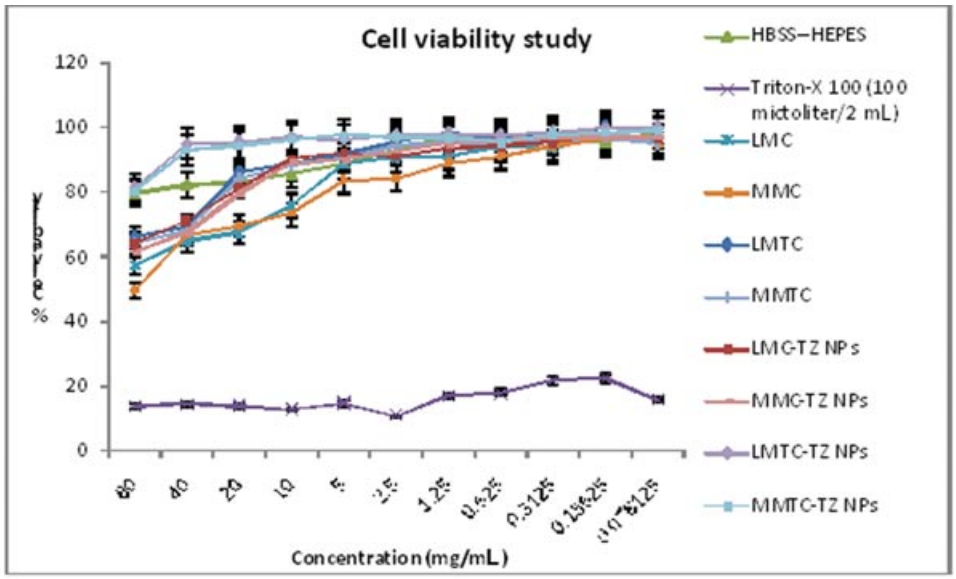


**(Mean ± S.D., $n$ = 3)**

LMC- low molecular weight chitosan
MMC- medium molecular weight chitosan
LMTC- low molecular weight thiolated chitosan
MMTC- medium molecular weight thiolated chitosan
LMC-TZ NPs- low molecular weight Tizanidine HCl loaded chitosan nanoparticles
MMC-TZ NPs-medium molecular weight Tizanidine HCl loaded chitosan nanoparticles
LMTC-TZ NPs- low molecular weight Tizanidine HCl loaded thiolated chitosan nanoparticles
MMTC-TZ NPs- medium molecular weight Tizanidine HCl loaded thiolated chitosan nanoparticles

**Figure 6.** Gamma scintigraphy images of (a) $^{99m}$TC–TZ solution (i.v.), (b) $^{99m}$TC–TZ solution (oral), (c) $^{99m}$TC–TZ solution (i.n.), (d) $^{99m}$TC–LMC-TZ NPs, (e) $^{99m}$TC–MMC-TZ NPs, (f) $^{99m}$TC–LMTC-TZ NPs, and (g) $^{99m}$TC–MMTC-TZ NPs.

(a) Biodistribution of TZ in Blood

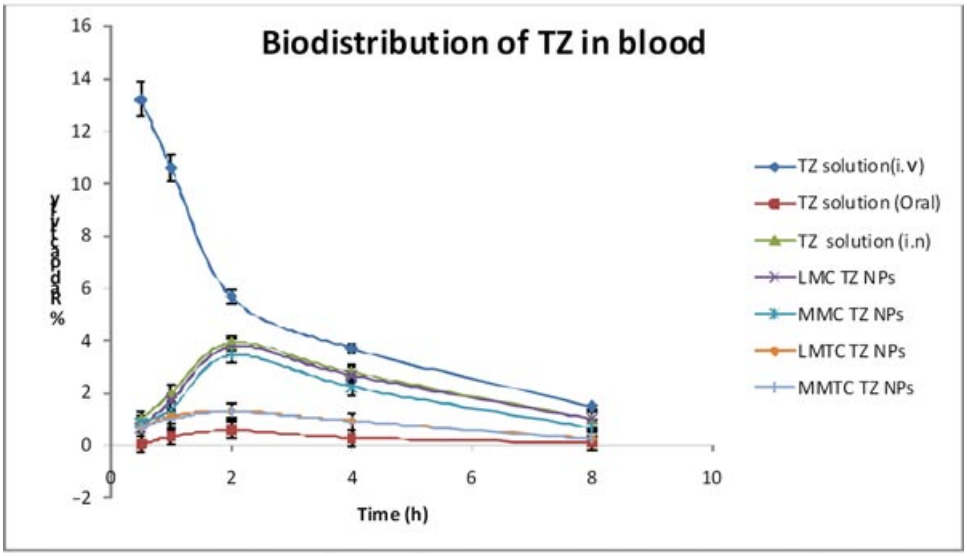


(b) Biodistribution of TZ in brain

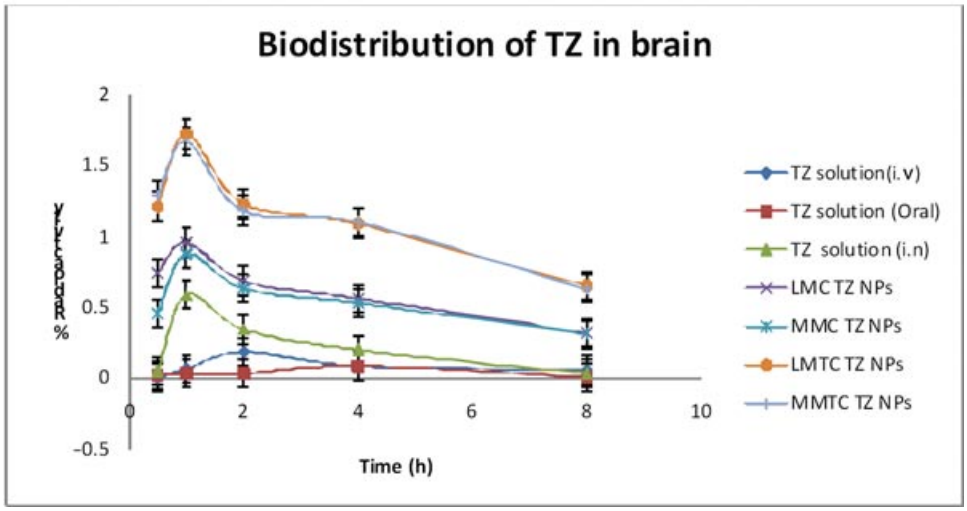


**Figure 7.** Antinociceptive effect of TZ formulations on mice hot plate test.

0.1 mm at the delivery site. For the comparison study, TZ solution equivalent to 0.00104 mg/g of TZ was administered via oral route. Hot plate method was used for the evaluation of antinociceptive effect. Mice were placed on the stainless steel plate and temperature was set at 55 ± 0.1°C. Reaction time was measured using stopwatch before and after the treatment. Licking of the fore of hind paws was considered the endpoint. The mice reaction time less than 12 s and more than 18 s before treatment were excluded from the study. An arbitrary cutoff was taken at 45 s.[25,26] Figure 7 shows the percent maximum possible effect (% MPE) of TZ formulations.

The results of hot plate method were evaluated by nociceptive thresholds for the hot plate test that converted to % MPE according to the following formula[27,28]:

$$\%\,\mathrm{MPE} = \frac{(\mathrm{Posttreatment\,value}) - (\mathrm{Pretreatment\,value})}{(\mathrm{Cutoff\,value}) - (\mathrm{Pretreatment\,value})} \times 100$$

When several groups were compared, statistical analysis was carried out using an initial one-way ANOVA. A $p$ value of less than 0.05 was considered significant.

## RESULTS AND DISCUSSIONS

### Preparation of TC

Thioglycolic acid was attached covalently to the primary amino groups on the surface of chitosan. The carboxylic acid moieties of TGA were activated using EDC and this reaction forms an intermediate

 DOI 10.1002/jps

*O*-acylurea derivative that can react with the primary amino groups of chitosan. To facilitate the optimization of TC synthesis, the influence of amount of chitosan–TGA and pH (pH 3–5) on amount of chitosan-immobilized thiol groups was evaluated during the coupling reaction. The pH of the coupling reaction has significant impact on the amount of TGA attached to chitosan. Amount of attached thiol group on the chitosan was comparatively low at pH 3 due to low reactive potential of EDC at pH 3. Hence, at pH 4, the amount of attached thiol group was significantly higher compared with pH 3 and lower than pH 5. Thiolation was maximum at pH 5 and above pH 5, the yield of polymer-bound thiol groups decreased again because of the oxidation of sulfhydryl groups during the coupling reaction, which is favored at higher pH values.[29,30] The effect of polymer to TGA ratio was also optimized during the coupling reaction at pH 5. Highest coupling was observed at 500 mg of polymer and 30 mL (39.6 g) of TGA.

### Preparation of TZ-Loaded Chitosan and TC NPs

Chitosan NPs with different molecular weights were prepared by ionic gelation of chitosan with SA, which involves the mixing of two aqueous solutions at ambient temperature while stirring without using sonication or organic solvents. Various formulations were made with different initial concentrations of chitosan (1, 1.5, and 2 mg/mL) and SA (0.5, 1, and 1.5 mg/mL) to establish preparation conditions at which NPs are formed. NPs generally show a higher uptake by nasal epithelia than microparticles.[31–34] The various factors such as particle size, particle size distribution, stability, and reproducibility of NPs were used to optimize the formulation parameters for preparation of NPs.[35] The optimal chitosan NPs were formed only when the ratio of chitosan solution (1 mg/mL) to SA solution (0.5 mg/mL) was 2:1. At lower or higher ratio of chitosan solution to SA solution, formation of clear solution and formation of larger NPs with low colloidal stability were obtained, respectively. Lower chitosan concentration (0.5 mg/mL) made encapsulation difficult and high concentration of chitosan (2 mg/mL) or SA (1.5 mg/mL) forms aggregates. The formation of NPs was possible only at moderate concentrations of chitosan and SA. As for ionotropic gelation between SA solution of 0.5 mg/mL and chitosan solution of 1–2 mg/mL, we generally observed opalescent suspension of NPs. With an increase in chitosan concentration, the %EE of drug decreases. It has been previously reported that the high viscosity of the gelation medium hinders the encapsulation of drug in case of chitosan microspheres.[36] So, it was assumed that lower the viscosity of chitosan, higher is the encapsulation of drug and gelation between chitosan and SA.[19]

With increase in the concentration of drug in optimal formulation (1, 2.5, and 4 mg/mL), drug entrapment increased but above 2.5 mg/mL it was found to decrease.[17] Entrapment efficiency of medium-molecular-weight chitosan was more than that of low-molecular-weight chitosan. These results are attributed to the longer polymer chains of medium-molecular-weight chitosan, which can encapsulate more drugs after gelation with SA.[19] The impact of chitosan solution pH (4 and 5) and SA pH (8, 9, 10, and 11) was observed on the particle size and drug entrapment of optimal formulations. Higher entrapment and lower size of NPs were found at pH 5 of chitosan solution and pH 9 of SA solutions. These findings suggest that when the pH of the polymers is adjusted to 5, the $NH_2$ groups of the chitosan are predominantly protonated and are better available for interaction.[18] With increase in pH of SA from 8 to 11, drug entrapment increased up to pH 9 and decreased above this pH. The influence of chitosan molecular weight on the particle size was evaluated and it was observed that with increase in molecular weight, the particle size also increases, as medium-molecular-weight chitosan can be more accessible for interaction and can entrap more drug as compared with low-molecular-weight chitosan. It is explained by the fact that medium-molecular-weight chitosan is comparatively less soluble than low-molecular-weight chitosan and as a result, increase in particle diameter and aggregation may be obtained.[19] Free amino group of the chitosan was responsible for the positive zeta potential values for all formulations, which might ensure the electrostatic interaction of positive charge of chitosan with the anionic charge of mucus.

Nanoparticles from TC with different molecular weight were prepared by ionic gelation of TC using SA with slight modification in aforementioned method. Different formulations were made with various concentrations of TC (1, 2, and 3 mg/mL) and SA solutions (0.25. 0.5, and 0.75 mg/mL). The lower concentration range (0.25. 0.5, and 0.75 mg/mL) of SA solution was selected for the formation of NPs because the formation of microparticles at higher range (above 0.75 mg/mL) was observed. The influence of low- or medium-molecular-weight TC to SA ratio was found to be similar as of chitosan NPs.[14] The impact of pH change on drug entrapment was negligible as thiolation increases positive charge and improves solubility of chitosan at physiological pH. Moreover, TZ was highly hydrophilic cationic drug, which has an effect on the drug entrapment with positively charged TC. The optimal TC NPs were formed when the TC (2 mg/mL) was dissolved in distilled water. Drug solution (2 mg/mL) incubated with anionic SDC (10 mg/mL) for 30 s leads to formation of neutral drug–SDC complex. The drug–SDC complex was added to TC solution. The addition of SA solution (0.5 mg/mL) with stirring to

the above mixture leads to the instant formation of NPs. The ratio of TC solution–SA solution–drug solution–SDC solution was selected as 7:1:1:1. It was found that with increase in the concentration of drug from 1 to 2 mg/mL in optimal formulation, entrapment was found to be increased and decreased thereafter. Moreover, with increase in the concentration of SDC up to 10 mg/mL, the drug entrapment increased because of the formation of neutral drug–SDC complexes, which adsorbed more on the positively charged TC in comparison with highly cationic drug.[16] As the concentration of SDC solution is increased, the size reduced and surface area increased. Hence, higher drug–SDC complex adsorption on the surface of TC leads to high drug entrapment. The mean hydrodynamic diameter of TC NPs increased with increasing molecular weight of TC, which conforms to previously reported works.[15,36]

## Characterizations

### Characterization of TC

*Procedure for Quantitating Sulfhydryl Groups Based on Molar Absorptivity (Ellman's Method).* The TC produced by carbodiimide exhibited 42.33 and 125.5 mmol immobilized free thiol groups per gram of low- and medium-molecular-weight polymer, respectively. The results indicate that the amount of covalently bound thiol groups can be increased as much as twice by preventing the oxidation of thiol groups.[9–11]

*Infrared Spectra.* The coupling of TGA to chitosan was confirmed by the presence of S–H group. The spectra from thiolated samples contained a peak in the thiol group range at 2550–2600 $cm^{-1}$, which indicated the presence of thiol group attached to the surface of chitosan, a peak that is not found in the spectrum of the unmodified chitosan. Figure 1 shows the infrared spectra of low- and high-molecular-weight chitosan and TC.

### Characterization of Chitosan and TC NPs

*Particle Size.* The mean particle size of TZ/RB-loaded chitosan and TC NPs were found to be in the range of 461–622 nm and 262–277 nm, respectively (Table 1).

*Zeta Potential.* The zeta potential of TZ/RB-loaded chitosan and TC NPs were found to be in the range of 21–25 mV and 12–19 mV, respectively (Table 1). Results of zeta potential demonstrated high positive (+30 mV) surface charge on NPs, which indicates higher stability because of the anticipated surface repulsion between similarly charged particles, thereby inhibiting aggregation of the colloidal particle. Positively charged particles are expected to have a higher residence time on negatively charged nasal mucosa.

*Encapsulation Efficiency or PDE.* The %EE of TZ/RB-loaded chitosan and TC NPs were found to be in the range of 40%–64% and 65%–76%, respectively (Table 1).

*Transmission Electron Microscopy.* Transmission electron microscopy micrograph showed that the TZ-loaded chitosan and TC NPs were found to be uniform particles in nanorange (Fig. 2).

### Confocal Laser Scanning Microscopy Examination

As observed by confocal laser scanning microscopy, the thiolated NPs and chitosan NPs have strong interaction on the nasal mucosa than the RB solution. Figure 3 shows the higher penetration of TZ-loaded TC NPs (Figure 3d and 3e) than chitosan NPs (Figure 3b and 3c) and RB solution (Fig. 3a). This bioadhesive effect resulted due to enhanced contact time by the formation of covalent bonds with the cysteine residues of the mucus glycoprotein with TC NPs. As a consequence of this, high concentration of drug on the absorption site promotes an effective permeation through the nasal mucosa, which might be due to the increased solubility of chitosan after thiolation. Images after the Z sectioning of nasal mucosa confirmed the higher permeation of RB from thiolated NPs than the chitosan NPs and RB solution. Increased order of mucoadhesion properties and permeability of RB through the nasal mucosa was indicated as medium-molecular-weight rhodamine B-loaded thiolated chitosan nanoparticles (MMTC-RB NPs)> low-molecular-weight rhodamine B-loaded thiolated chitosan nanoparticles (LMTC-RB NPs) > medium-molecular-weight rhodamine B-loaded chitosan nanoparticles (MMC-RB NPs)> low-molecular-weight rhodamine B-loaded chitosan nanoparticles (LMC-RB NPs) > RB solution.[20] Figure 3 shows the confocal image of mucosal surface and Figure 4 shows the confocal image of after Z sectioning of nasal mucosa for RB solution and RB-loaded chitosan/TC NPs.

### TEER Measurement and Permeation Studies of TZ Solution and TZ-Loaded Chitosan and TC NPs

Transepitheial electrical resistance was measured for TZ solution and TZ-loaded NPs formulations at different time intervals. TZ solution showed a negligible change from the initial TEER value during the incubation of cells up to 150 min. In case of TZ-loaded chitosan NPs and TZ-loaded TC NPs, the initial TEER value starts to decrease at 30 min and continued decreasing up to 150 min. TZ-loaded TC NPs showed a significant ($p < 0.05$) reduction in TEER than the TZ

solution and chitosan NPs.[37] TEER of TZ formulations is recorded in Table 2.

Upon incubation with TZ-loaded chitosan NPs for 150 min, there was an irreversible decrease in TEER. This could be due to destruction of the tight junctions of the RPMI 2650 cell monolayer. This might be due to the higher cytotoxicity of chitosan NPs than the TC NPs.[22] TC has an ability to decrease the initial TEER that can be explained by reversible opening of the tight junction.[37]

Permeation of TZ across the RPMI 2650 cell monolayer determines AP to BL direction. $P_{app}$ of TZ solution, TZ-loaded chitosan, and TZ-loaded TC NPs was measured and recorded in the Table 3. $P_{app}$ of TZ solution was found to be $0.674 \pm 0.032 \times 10^6$ cm/s. TZ-loaded TC NPs shows a significantly ($p < 0.05$) higher $P_{app}$ value than chitosan NPs and TZ solution across the RPMI 2650 cell monolayer. $P_{app}$ of TZ-loaded TC NPs and chitosan NPs was found to be 29-fold and 13-fold higher than the TZ solution, respectively. $P_{app}$ of TZ formulations across the RPMI 2650 cell monolayer is graphically shown in Figure 8. Significantly high permeation of drug from the TC was associated with the inhibition of CYP450 enzyme activity, which was responsible for the metabolism of TZ across the nasal mucosa. The inhibition of CYP450 activity across the mucosa by nonabsorbable thiol group containing compound such as TC seems to be based on the formation of disulfide bond between the cysteine-rich subdomains of the mucus glycoproteins and TC and attachment of thiol group of TC with the CYP450 enzymes across the nasal mucosa via disulfide bonds across the nasal mucosa by utilizing the flavoprotein NADPH–P450 reductase electrons that make CYP450 enzymes inactive for metabolism due to unavailability of reducing environment.[38]

### *Cell Viability Study*

Influence of soluble chitosan, soluble TC, chitosan NPs, and TC NPs on the RPMI 2650 nasal epithelial cells is shown in Figure 5. The toxicity of TC NPs suspension (40 mg/mL) and soluble TC (20 mg/mL) was found to be nonsignificant ($p < 0.05$), which may be due to the covalent and reversible binding of polymer with the nasal epithelial cells. We observed a decrease in cell viability with soluble TC at relatively high concentration of 40 mg/mL ($p < 0.001$). The Triton-X 100 (50 μL/mL) was chosen as positive control. To illustrate the safety of TC, its effect on the cell viability was directly compared with that of Triton-X 100. A substantial decrease in the cell viability was observed after incubation with Triton-X 100 compared with HBSS–HEPES ($p < 0.001$). Chitosan NPs suspension (10 mg/mL) and soluble chitosan (5 mg/mL) showed less cell viability compared with TC NPs suspension and soluble TC. The noncovalent and irreversible binding of polymer with the nasal epithelial cells lead to higher cytotoxicity of chitosan and chitosan NPs compared with TC and its NPs. Soluble chitosan also shows less cell viability compared with the chitosan NPs suspension. The high cell viability of TC NPs may be explained by increased solubility of chitosan after thiolation at physiological pH, resulting in quicker removal from the site of application while forming intimate contact with the mucosae because of covalent linkage. Hence, transmucosal drug delivery will be improved because of required retention of thiolated NPs on nasal mucosae. But they undergo complete removal from the mucosae through mucociliary clearance; improve safety, which is otherwise problem with the chitosan; and are a contributing factor to chitosan's nasal mucosal toxicity.[22]

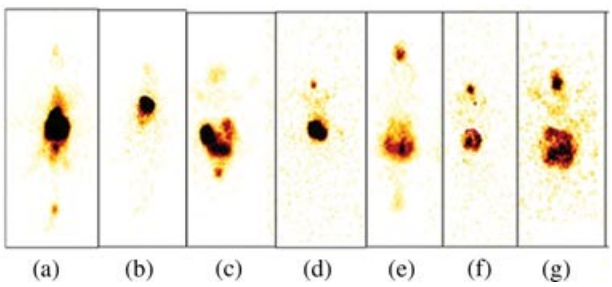


**Figure 8.** Apparent permeability coefficient ($P_{app}$) of TZ formulations across the RPMI 2650 cell monolayer.

## *In Vivo* Study

### *Biodistribution Studies*

TZ solution, chitosan NPs, and TC NPs were effectively radiolabeled with $^{99m}$Tc, optimized for maximum labeling efficiency and stability. The incubation time was optimized at 30 min. The pH for all the formulations was kept at around 6.5. The labeling efficiency and the stability of labeled complex were ascertained by ascending ITLC. Radiochemical purity of TZ solution, LMC-TZ NPs, MMC-TZ NPs, LMTC-TZ NPs, and MMTC-TZ NPs was found to be 97%, 97.5%, 97.9%, 99.2%, and 98.5%, respectively. The results suggested high stability of $^{99m}$Tc–TZ solution/LMC-TZ NPs/MMC-TZ NPs/LMTC-TZ NPs/MMTC-TZ NPs. The stability studies of $^{99m}$Tc-labeled TZ were carried out *in vitro* using normal saline and mice serum by ascending ITLC. The stability of complexes was carried out for 24 h. The bonding strength of $^{99m}$Tc-labeled TZ formulations was assessed by DTPA challenging test. The influence of different molar concentration of DTPA on $^{99m}$Tc-labeled TZ and percentage transchelation was studied. The percentage transchelation of the labeled complex was found to be below 4% (w/w) for all formulations at highest concentration (50 mM). The results of

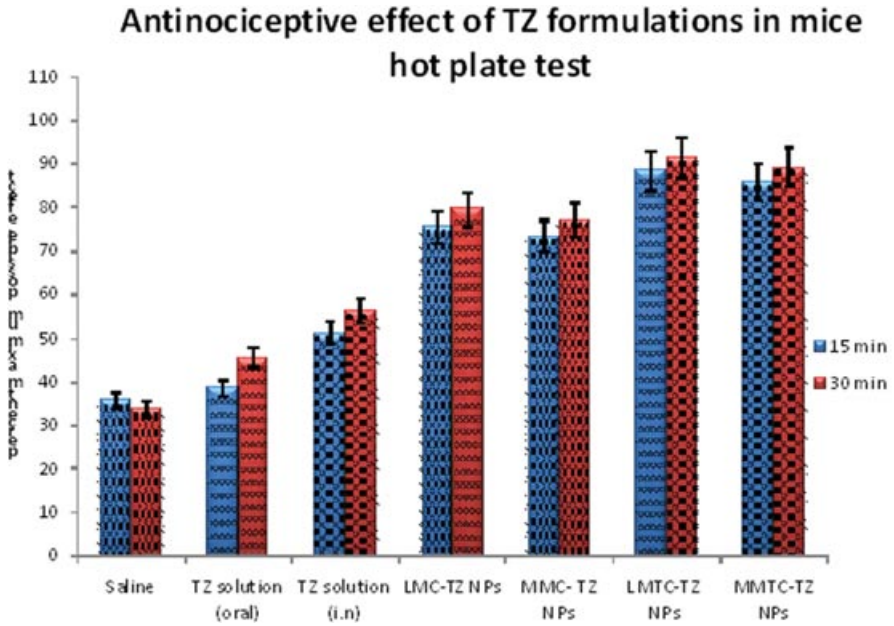


**Figure 9.** Blood and brain concentration versus time plot following administration of $^{99m}$TC–TZ formulations. (a) biodistribution of TZ in blood and (b) biodistribution of TZ in brain.

these findings suggest high bonding strength and stability of $^{99m}$Tc-labeled drug, thus these formulations were found suitable for biodistribution studies of the drug in Swiss albino mice. Biodistribution of $^{99m}$Tc–TZ formulations following i.v., oral, and i.n. ($^{99m}$Tc–TZ solution/LMC-TZ NPs/MMC-TZ NPs/LMTC-TZ NPs/MMTC-TZ NPs) administration on Swiss albino mice was studied and the percentage radioactivity per gram of tissue/organ was determine at predetermined time intervals up to 8 h. The results of the brain–blood ratio of the drug at all time points for all formulations were also calculated and tabulated in Table 4. The pharmacokinetic parameters derived from Figures 9a and 9b for all formulations were recorded in Table 5. $^{99m}$Tc–TZ-labeled TZ in solution/chitosan NPs/TC NPs show low $T_{max}$ value in brain (around 1 h) after nasal administration as compared with blood (around 2 h) (Table 5). Intranasal-administered $^{99m}$Tc-labeled TZ formulations showed high brain–blood ratios of the TZ as compared with oral and i.v. administration (Table 4). These findings confirmed the direct nose-to-brain transport. Significantly higher uptake of $^{99m}$Tc–TZ-labeled TZ (solution/NPs formulation) in brain via i.n. administration was found at all time points compared with $^{99m}$Tc-labeled TZ solution alone following i.v. and oral administration up to 8 h. These results may be recognized by the higher mucoadhesion capacity of i.n. administered chitosan and TC NPs on nasal mucosa, which significantly improves the drug transport by enhancing the residence time of formulations on nasal mucosa compared with the TZ solution (i.v.) and TZ solution (oral). Higher brain uptake of TZ was found in $^{99m}$Tc-labeled TC NPs via i.n. route than the $^{99m}$Tc-labeled chitosan NPs. These results may be due to higher mucoadhesive strength of TC than the chitosan. These results may be associated with increase in solubility at physiological pH, which leads to faster absorption from site of administration.[24]

The significantly high uptake of NPs in the brain through i.n. route suggests a higher selective transport of TZ into the brain.[39,40] The range of $T_{1/2}$ with all formulations were found to be 2.25–3.08 h in blood and 1.75.2–6.38 h in brain, irrespective of the factors such as type of formulations and administration. After i.n. administration, high value of $C_{max}$ and AUC was found with $^{99m}$Tc-labeled TC NPs compared with $^{99m}$Tc-labeled chitosan NPs and TZ solution. These results may be explained by improved mucoadhesion after thiolation of chitosan on nasal mucosa, resulting in prolonged contact time of the formulation with the nasal mucosa. The DTI and brain drug direct transport percentage [DTP (%)] were calculated for nasally administered formulations and are shown in Table 5. The $^{99m}$Tc-labeled TC NPs showed the highest DTI and DTP (%) than the $^{99m}$Tc-labeled chitosan NPs and TZ solution. These higher values of DTI and DTP (%) show the advantage of the TC NPs for i.n. administration. The higher DTI and DTP (%) advocate improved brain targeting efficiency of TC NPs due to considerable direct nose-to-brain transport.[39]

### *Gamma Scintigraphy Imaging*

Gamma scintigraphy study was performed for $^{99m}$TC–LMC-TZ NPs/MMC-TZ NPs/LMTC-TZ NPs/MMTC-TZ NPs/$^{99m}$TC–TZ solution in Swiss albino mice. To visualize the location of drug into the brain following i.n., oral, and i.v. administrations of $^{99m}$Tc–TZ solution/chitosan NPs/TC NPs, we used a gamma scintigraphy camera to obtain absolute biodistribution of TZ. The gamma scintigraphy images in Swiss albino mice were taken 15 min after i.v. injection, oral and i.n. administrations (Fig. 6). Figure 6 shows the presence of radioactivity in the area of esophagus via i.n. route due to carry over of a part of the formulations toward gastrointestinal tract. The scintigraphy images were found consistent with the results shown in Table 4 and high brain uptake of TC NPs into the brain was observed than the chitosan NPs and TZ solution when administered via i.n. route.[37,39]

### *Pharmacodynamic Study*

Results of the hot plate method were graphically shown in Figure 7. Results shows that the antinociceptive effect of i.n.-administered TZ formulations was significantly higher ($p < 0.05$) than the oral administration of TZ solution after 30 min. TZ-loaded TC NPs show significantly high antinociceptive effects than the TZ-loaded chitosan NPs. These findings may be due to the high mucoadhesion and permeation capacity of TC than the chitosan. High permeation of TC was due to improvement of solubility at physiological pH after thiolation. Intranasal TZ solution shows significantly lower antinociceptive effect than the NPs formulations. Theses results may be explained by the reversible opening of the paracellular route for hydrophilic molecules so that more drug can be absorbed through nasal mucosa.[26]

## CONCLUSION

The findings of this investigation accrued into interesting and therapeutically beneficial chitosan derivative, TC, for nose to brain drug delivery. TC was used to prepare NPs of TZ, and significantly higher drug brain uptake and pain alleviation activity were observed after intranasal administration compared with drug chitosan NPs. After thiolation, the recovery of tight junction was observed to be faster and complete between two dosing, which was otherwise causing toxicity due to incomplete reversal with chitosan, keeping in the mind that hydrophilic drug, such as TZ, does not cross BBB effectively or have erratic brain pharmacokinetics. In this investigation, we incorporated hydrophilic drug into TC and improved brain uptake of drug, which was otherwise known for erratic pharmacokinetic after oral administration. Another reason for improved brain drug uptake may be because of the inhibition of CYP450 activity across the mucosa by the attachment of thiol group with the CYP450 enzymes across the nasal mucosa via disulfide bonds by utilizing the flavoprotein NADPH–P450 reductase electrons that make CYP450 enzymes inactive for metabolism because of unavailability of reducing environment. However, these benefits have to be confirmed by studies in one more animal species with special emphasis on toxicity to nasal mucosa, followed by clinical evaluation to ascertain the clinical use of TC.

## ACKNOWLEDGMENTS

The authors acknowledge the financial assistance from Funding agency of research scholar and TIFAC CORE in NDDS, Government of India, New Delhi, for providing the research facilities to the team; AICTE for providing Deepa Patel "National doctoral fellowship." Authors heartily gratified to Dr. A. K. Mishra for providing the facility for radiolabeling study and Dr. Rashi Mathur, Mrs. Krishna Chttani, Dr. N.K. Chaudhari, Mr. Athar, and Mr. Amit for their help during my work at Institute of Nuclear Medicine and Allied Sciences, Delhi, India.

## REFERENCES

1. Fogelholm R, Murros K. 1992. Tizanidine in chronic tension-type headache: A placebo controlled double-blind cross-over study. Headache 32:509–513.
2. Berry H, Hutchinson DR. 1988. Tizanidine and ibuprofen in acute low-back pain: Results of a double-blind multicentre study in general practice. J Int Med Res 16:83–91.
3. Soane RJ, Hinchcliffe M, Davis SS, Illum L. 2001. Clearance characteristics of chitosan based formulation in the sheep nasal cavity. Int J Pharm 21:183–191.
4. Desai M, Labhasetwar V, Amidon GL, Levy RJ. 1996. Gastrointestinal uptake of biodegradable microparticles: Effect of particle size. Pharm Res 13:1838–1845.
5. Aston R, Saffie-Siebert R, Canham L, Ogden J. 2005. Nanotechnology application for drug delivery. J Pharm Technol Eur 17:21–28.
6. Illum L. 1998. Chitosan and its use as a pharmaceutical excipient. Pharm Res 15:1326–1331.
7. Borchard G, Lueßen HL, de Boer AG, Verhoef JC, Lehr CM, Junginger HE. 1996. The potential of mucoadhesive polymers in enhancing intestinal peptide drug absorption: III. Effects of chitosan glutamate and carbomer on epithelial tight junctions *in vitro*. J Controlled Release 39:131–138.
8. Lee KY, Ha WS, Park WH. 1995. Blood compatibility and biodegradability of partially N-acylated chitosan derivatives. Biomaterials 16:1211–1216.
9. Kotze AF, Luehen HL, de Leeuw BJ, de Boer AG, Verhoef JC, Junginger HE. 1999. Chitosan for enhanced intestinal permeability: Prospects for derivatives soluble in neutral and basic environments. Eur J Pharm Sci 7:145–151.
10. Snyder GH, Reddy MK, Cennerazzo MJ, Field D. 1983. Use of local electrostatic environments of cysteines to enhance

formation of a desired species in a reversible disulfide exchange reaction. Biochim Biophys Acta 749:219–226.
11. Sreenivas SA, Pai KV. 2008. Thiolated chitosans: Novel polymers for mucoadhesive drug delivery—A review. Trop J Pharm Res 7:1077–1088.
12. Andreas BS, Hornof M, Zoidl T. 2003. Thiolated polymers—Thiomers: Modification of chitosan with 2-iminothiolane. Int J Pharm 260:229–237.
13. Hornof MD, Kast CE, Andreas BS. 2003. *In vitro* evaluation of the viscoelastic behavior of chitosan—Thioglycolic acid conjugates. Eur J Pharm Biopharm 55:185–190.
14. Dong-Won L, Shawna AS, Richard FL, Shyam SM. 2006. Thiolated chitosan nanoparticles enhance anti-inflammatory effects of intranasally delivered theophylline. Respir Res 7:112.
15. Worawan B, Hans EJ, Neti W, Assadang P, Tasana P. 2008. Preparation and characterization of particles from chitosan with different molecular weights and their trimethyl chitosan derivatives for nasal immunization. J Met Mater Miner 18:59–65.
16. Carmen P, Hayat O. 2009. Biodegradable nanoparticles incorporating highly hydrophilic positively charged drugs. Patent US424489.
17. Wang X, Chi N, Tang X. 2008. Preparation of estradiol chitosan nanoparticles for improving nasal absorption and brain targeting. Eur J Pharm Biopharm 70:735–740.
18. Sadeghi AMM,Dorkoosh FA, Avadi MR, Saadat P, Rafiee-Tehrani M, Junginger HE. 2008. Preparation, characterization and antibacterial activities of chitosan, *N*-trimethyl chitosan (TMC) and *N*-diethylmethyl chitosan (DEMC) nanoparticles loaded with insulin using both the ionotropic gelation and polyelectrolyte complexation methods. Int J Pharm 355:299–306.
19. Yan W, Wuli Y, Changchun W, Jianhua H, Shoukuan F. 2005. Chitosan nanoparticles as a novel delivery system for ammonium glycyrrhizinate. Int J Pharm 295:235–245.
20. Law SL, Huang KJ, Chou HY. 2001. Preparation of desmopressin-containing liposomes for intranasal delivery. J Controlled Release 70:375–382.
21. Bai S, Yang T, Abbruscato TJ, Ahsan F. 2008. Evaluation of human nasal RPMI 2650 cells grown at an air–liquid interface as a model for nasal drug transport studies. J Pharm Sci 97:1165–1178.
22. Maryam A, Stefan GR, Gerrit B, Hans EJ, Wim EH, Wim J. 2006. Preparation and characterization of protein-loaded N-trimethyl chitosan nanoparticles as nasal delivery system. J Controlled Release 111:107–116.
23. Shah P, Jogani V, Mishra P, Mishra AK, Bagchi T, Misra AN. 2008. *In vitro* assessment of acyclovir permeation across cell monolayers in the presence of absorption enhancers. Drug Dev Ind Pharm 34:279–288.
24. Vyas TK, Babbar RK, Sharma S, Misra AN. 2006. Intranasal mucoadhesive microemulsions of clonazepam: Preliminary studies on brain targeting. J Pharm Sci 95:1–11.
25. Ghelardini C, Galeotti N, Grazioli I, Uslenghi C. 2004. Indomethacin, alone and combined with prochlorperazine and caffeine, but not sumatriptan, abolishes peripheral and central sensitization in *in vivo* models of migraine. J Pain 5:413–419.
26. Langerman L, Zakowski MI, Piskoun B, Grant GJ. 1995. Hot plate versus tail flick: Evaluation of acute tolerance to continuous morphine infusion in the rat model. J Pharmacol Toxicol Meth 34:23–27.
27. Schreiber S, Backer MM, Pick CG. 1999. The antinociceptive effect of venlafaxine in mice is mediated through opioid and adrenergic mechanisms. Neurosci Lett 273:85–88.
28. Sawynok J, Esser MJ, Reid AR. 1999. Peripheral antinociceptive actions of desipramine and fluoxetine in an inflammatory and neuropathic pain test in the rat. Pain 82:149–158.
29. Bernkop-SchnuK A, Scholler S, Biebel RG. 2000. Development of controlled drug release systems based on thiolated polymers. J Controlled Release 66:39–48.
30. Kast CE, Bernkop-Schnürch A. 2001. Thiolated polymers—Thiomers: Development and *in vitro* evaluation of chitosan thioglycolic acid conjugates. Biomaterials 22:2345–2352.
31. Agnihotri SA, Mallikarjuna NN, Aminabhavi TM. 2004. Recent advances on chitosan-based micro- and nanoparticles in drug delivery. J Controlled Release 100:5–28.
32. Delie F. 1998. Evaluation of nano- and microparticle uptake by the gastrointestinal tract. Adv Drug Del Rev 34:221–233.
33. Huang Y, Donovan MD. 1998. Large molecule and particulate uptake in the nasal cavity: The effect of size on nasal absorption. Adv Drug Del Rev 29:147–155.
34. Brooking J, Davis SS, Illum L. 2001. Transport of nanoparticles across the rat nasal mucosa. J Drug Target 9:267–279.
35. Fernández-Urrusuno R, Calvo P, Remuñan-López C, Vila-Jato JL. 1999. Enhancement of nasal absorption of insulin using chitosan nanoparticles. J Pharm Res 16:1576–1581.
36. Vandenberg GW, Drolet C, Scott SL, de la Noüe J. 2001. Factors affecting protein release from alginate-chitosan coacervate microcapsules during production and gastric/intestinal simulation. J Controlled Release 77:297–307.
37. Wengst A, Reichl S. 2010. RPMI 2650 epithelial model and three-dimensional reconstructed human nasal mucosa as *in vitro* models for nasal permeation studies. Eur J Pharm Biopharm 74:290–297.
38. Iqbal J, Sakloetsakun D, Bernkop-Schnürch A. 2011. Thiomers: Inhibition of cytochrome P450 activity. Eur J Pharm Biopharm 78:361–365.
39. Illum L. 2000. Transport of drugs from the nasal cavity to central nervous system. Eur J Pharm Sci 11:1–18.
40. Thorne RG, Pronk GJ, Padmanabhan V, Frey WH. 2004. Delivery of insulin-like growth factor-I to the rat brain and spinal cord along olfactory and trigeminal pathways following intranasal administration. Neuroscience 127:481–496.